

Trotterization in universal quantum simulators under faulty control

George C. Knee* and William J. Munro
*NTT Basic Research Laboratories, NTT Corporation,
 3-1 Morinosato-Wakamiya, Atsugi, Kanagawa 243-0198, Japan*
 (Dated: December 3, 2024)

A universal quantum computer can be made to mimic the dynamics of any physical system, a feat possible on classical machines only with significant approximations or mean-field methods. Use of the Trotter formula is central to this endeavour: by repeatedly simulating a series of component evolutions, in principle it allows for the quantum computer to be efficiently driven arbitrarily close to an ideal time evolution described by a piecewise-local Hamiltonian. Here we show that the ability to reduce the simulation error (which we quantify in a variety of ways, including with the diamond norm) at will (theoretically achieved by increasing the number of control gates per unit time) is lost when finite imperfections in the control of the quantum computer are introduced. The imperfections thus set a bound in the accuracy of the simulation and on the maximum simulation time. We provide analytical results and numerical data exploring these limits and suggestions on how to achieve them in the laboratory. Our investigations indicate the optimum number of Trotter steps to employ.

I. INTRODUCTION

The purpose of a simulation is to learn something about a system of interest, or *simuland*, through the control and study of an entirely separate system: the simulator. The motivation for simulations arises because of the high controllability and efficiency of purpose built simulating machines: in modern times these are almost exclusively digital computers. Exploiting, as they do, GHz processor clock rates and memory registers boasting GB or TB or storage capacities, digital computers can be made to simulate a huge variety of physical systems such as weather, nuclear reactions, genetic mutations, and so on. Parameters are modified at will, so that different scenarios can be explored with any desired precision. The limits of such simulations, arising from the number of transistors in an integrated circuit, have been extended twofold approximately biennially since the 1970s, a trend known as Moore's law [1]. When the simuland is such that a fully quantum mechanical model is necessary to describe it, however, even continued improvement under Moore's law will not permit simulations on a digital computer for systems above a certain size. The memory requirement scales exponentially in the particle number. This problem can be overcome by moving to quantum simulation.

Examples of simulands exhibiting the quantum scaling problem include atomic or molecular systems (the subject of quantum chemistry simulations [2]) and condensed matter systems described by (for example) the Hubbard [3], Ising [4] or Heisenberg model [5]. A quantum simulator, on the other hand, is typically constructed with two-level systems known as 'qubits'. Such quantum-information-carrying elements may be realised with trapped ions [4], superconducting circuits [3, 6], or other candidate systems [7]. One can efficiently represent the quantum state of the simuland by storing an

image of it in the memory of the quantum simulator. To simulate dynamics, one assumes access only to a discrete set of control operations: for example single qubit 'rotations' along with an entangling gate such as a controlled-NOT [8]. Such a collection of control operations is known to enable universal quantum computation [9–11] – digital quantum simulators are therefore thought of as quantum computers [12]. Analogue quantum simulators are a rather different proposition: they skirt the issue of controllable dynamics by directly engineering a fixed global Hamiltonian. The disadvantages are limited reprogrammability and lack of error correction – see e.g. [13].

Quantum simulation is composed of preparation, evolution and readout stages. The aim of this paper is to quantify the accuracy of the evolution stage of digital quantum simulation given imperfect control. Analyses concerning state preparation and data extraction can be found elsewhere [14, 15].

The problem of noise in quantum computers has, in one sense, been solved by the error-correction threshold theorems [16–19]. An error correction threshold is a critical value of a measure of the accuracy of quantum control. Once it has been surpassed, error correction techniques work to decrease the overall net error. These theorems show that, when experimental operations become clean enough, encoding logical qubits in a larger number of redundant physical qubits allows the error in the overall computation to be suppressed at will [20]. But as interest in simulators grows [21], and small scale (say 64 qubit) devices begin to appear, the noise problem remains until many-thousand-qubit devices can be engineered so that full fault tolerance is possible. Even after fault tolerance is available, the question of how the overall computation depends on the *logical* (i.e. error-corrected) error rate is of fundamental importance.

* gk@physics.org

II. SIMULATION ALGORITHM

Even when a universal gate set is available, one does not generally know how to combine the gates *efficiently* to achieve a particular evolution of the quantum computer. Lloyd's algorithm [22] is a general but approximate solution to this problem, when the desired evolution is known to be generated by a local Hamiltonian:

$$H = \sum_{j=1}^k H_j, \quad (1)$$

where each of the k component Hamiltonians H_j has dimension less than some maximum (call this g). The true evolution is then approximated through a truncation of the Trotter [23] formula:

$$U = \exp[iHt] = \left(\prod_{j=1}^k \exp[iH_j t/n] \right)^n + \dots \quad (2)$$

where we set $\hbar = 1$, and take H to be time independent (although this can be straightforwardly relaxed).

The advantage of Lloyd's approach is that the number of operations required is reduced from being exponential in the particle number to being bounded by a number proportional to $t^2 kg^2/\epsilon$, where t is the simulation time, g is the maximum dimension of the local Hamiltonians, and ϵ is the desired error [24]. The total number k of component Hamiltonians has a better-than-polynomial (rather than exponential) dependence on the particle number, making Lloyd's method 'efficient'.

It is clear that for any finite value of n (the 'Trotter number'), the higher order terms in the above equation will be non-zero. Their neglect then necessarily leads to an error in the simulation - the simulator is not driven to the desired final state but to one that is nearby. As we shall see, 'nearby' can be given a concrete mathematical and operational definition.

Higher Trotter numbers result in trajectories of the simulator that result in a final state that is closer to the ideal. Increasing n will generally increase the computational complexity - more control operations. More time may not be required, however, because the gates are correspondingly shorter: although it is not clear if this carries over to the error corrected case. Others have considered the dependence of the number of gates and simulation time on the desired error [25], but here our only concern is the overall accuracy of the simulation. Higher order approximants are available [26, 27], or other techniques that exploit sparsity [28]. The common attributes of these approaches are that they reduce the number of operations to polynomial in the particle number, and that their accuracy is controlled (improved) by increasing the number of applied operations. The number of Trotter steps necessary for quantum chemistry simulation was considered by [29] and the number of gates estimated in [30].

Throughout this paper we take $V_j = \exp[iH_j t/n]$ as primitive operations applied to the simulator, although ultimately these primitives should be understood as being composed from gates drawn from the particular universal set that is available.

III. TIME-ENERGY FREEDOM

Because of the $H \rightarrow aH, t \rightarrow t/a$ symmetry of the Schrödinger equation $i\frac{\partial}{\partial t}|\psi\rangle = -H|\psi\rangle$, when simulating closed-system dynamics one benefits from the freedom to define

$$\begin{aligned} H_{\text{simulator}} &= aH_{\text{simuland}} \\ t_{\text{simulator}} &= \frac{1}{a}t_{\text{simuland}}, \end{aligned} \quad (3)$$

which will preserve the correspondence between the time evolutions of the simulator and simuland. The simulation time, therefore, may be chosen to be any duration as long as the appropriate global scaling of the energy of the control fields is also performed. Even classical simulators are rarely operated at a speed commensurate with their respective simulands - weather patterns of several weeks are simulated in a matter of hours, and supercomputers spend months calculating chemical reaction dynamics over timescales many orders of magnitude smaller. In fact, because each unitary $\exp[iH_j t/n]$ is decomposed into the natural elementary gate set of the simulator, one generally expects a non unit effective value for a . Clearly this freedom enables the computation to be sped up (or slowed down) by a constant factor [31], but more importantly we imagine that such freedom may prove very useful for reducing noise in implementations of quantum simulation, depending on the particular noise which dominates - see below. It is worth noting that assuming this freedom is more than is necessary for universal quantum computation - nevertheless in many quantum computers we expect there to be at least a limited ability to perform the primitive operations at different physical speeds.

IV. NOISE TYPES

The error in approximating the true evolution with the first term on the RHS of (2) is known to decay at worst as $\propto n^{-1}$ [32], and as Lloyd put it 'n can always be picked sufficiently large to ensure the simulator tracks the correct time evolution to within any [desired nonzero accuracy]' [22]. The perfect control of any system (quantum or classical) is only ever an idealisation however. Precious little is known about the real-world situation - although the Trotter formula has recently shown to be stable under the right conditions [33]. Ref. [34] is a study of the influence of noise on certain quantum simulations, calculating the average fidelity of the final state of the computer with the ideal. Here we derive analytical results for arbitrary

(generally non-unitary and non-commuting) component Hamiltonians. Further, as we shall show, our results allow us to predict the ultimate performance of a faulty quantum simulator, and allow us to prescribe the optimum Trotter number to employ. Our results hold for a whole class of statistical distance metrics, including the most interesting *worst-case* metrics.

We construct ‘faulty Trotterized quantum channels’, and consider the following generalised noise map, with $\mathcal{V}_j(\rho) = e^{iH_j t/n} \rho e^{-iH_j t/n}$ representing the component unitary processes of Trotterization (here describing the transformation of a density matrix ρ describing the quantum state of the simulator):

$$\begin{aligned}\mathcal{E}^{\text{faultyTrotter}}(\rho) &= \bigcirc_{i=1}^n \bigcirc_{j=1}^k \mathcal{E}_{ij} \circ \mathcal{V}_j(\rho) \\ &= \bigcirc_{i=1}^n (\dots \circ \mathcal{E}_{i2} \circ \mathcal{V}_2 \circ \mathcal{E}_{i1} \circ \mathcal{V}_1)(\rho) \\ &= \bigcirc_{i=1}^n \mathcal{E}_i^{\text{fTss}}(\rho)\end{aligned}\quad (4)$$

The \circ symbol is used here to denote the concatenation of quantum channels: here we have a triple concatenation (first due to faulty evolutions \mathcal{E}_{ij} following the clean ones; second due to applying each of the k local Hamiltonians in turn, and third by repeating this process n times). The interleaved operations \mathcal{E}_{ij} are unwanted evolutions; they carry an index i to emphasise that they may vary over the course of the experiment, and there may also be a dependence on $\{H_j\}$, t and n . In the course of our derivations it is useful to consider the map over a single Trotter iteration (faulty Trotter single step) $\mathcal{E}_i^{\text{fTss}}$.

It will be convenient to consider the supermatrix representation of these maps: this is defined by $\mathbf{T}_{\mathcal{E}} \vec{\rho} = \overrightarrow{\mathcal{E}}(\rho)$, where $\vec{\rho}$ is the vectorized (column-stacked) density matrix and $\mathbf{T}_{\mathcal{E}}$ is a supermatrix of dimension d^2 . This representation makes the semigroup structure of quantum maps apparent. The concatenation of channels is merely matrix multiplication:

$$\begin{aligned}\mathbf{T}^{\text{faultyTrotter}} &= \prod_{i=1}^n \prod_{j=1}^k \mathbf{T}_{\mathcal{E}_{ij}} \mathbf{T}_{\mathcal{V}_j} \\ &= \prod_{i=1}^n (\dots \mathbf{T}_{\mathcal{E}_{i2}} \mathbf{T}_{\mathcal{V}_2} \mathbf{T}_{\mathcal{E}_{i1}} \mathbf{T}_{\mathcal{V}_1}) \\ &= \prod_{i=1}^n \mathbf{T}_i^{\text{fTss}}.\end{aligned}\quad (5)$$

We write the perfect implementation of the Trotter technique as \mathcal{V} with unitary matrix $V = (\sqrt[n]{V})^n$ and supermatrix $\mathbf{T}_{\mathcal{V}} = (\sqrt[n]{\mathbf{T}_{\mathcal{V}}})^n$ – essentially by removing all the faulty maps from the faulty Trotter channel.

We write the supermatrix representation of the ideal map \mathcal{U} as $\mathbf{U} = U \otimes U^*$, and break up this unitary evolution as

$$\mathcal{U}(\rho) = \bigcirc^n \sqrt[n]{\mathcal{U}}(\rho) \quad (6)$$

with the notation justified by the supermatrix describing each ideal Trotter step $\mathbf{U} = (\sqrt[n]{\mathbf{U}})^n$.

V. STATISTICAL DISTANCE MEASURES FOR QUANTUM CHANNELS

Hauke et al. pose the question – can we trust quantum simulators? [35]. Rather than give a binary answer, one can instead ask the question ‘to what extent can we trust quantum simulators?’ We aim to provide an answer to the above question in the form of a discrimination probability. To measure the faithfulness of quantum operations, one can appeal to generalisations of either classical fidelity or classical statistical distance between probability distributions. We prefer the latter here: the *trace distance* between quantum *states* (density matrices) has an operational meaning because it determines the success probability for the state discrimination problem [36]. One is provided with either ρ_A or ρ_B with equal probability and is asked to guess which after a single measurement. The probability of success is

$$p_{\text{distinguish}} = \frac{1}{2} + \frac{1}{4} \|\rho_A - \rho_B\|. \quad (7)$$

Here

$$\begin{aligned}\|\rho_A - \rho_B\| &= \text{Tr}|\rho_A - \rho_B| \\ &= \text{Tr}\sqrt{(\rho_A - \rho_B)(\rho_A - \rho_B)^\dagger}.\end{aligned}\quad (8)$$

The norm of the difference between the operators is a metric, giving the the quantum statistical distance between the operators. This definition implies that the discrimination is informed by measurement results arising from the optimum choice of POVM, or generalised measurement procedure. In fact

$$\|\rho_A - \rho_B\| = 2 \max_E \text{Tr}(E(\rho_A - \rho_B)). \quad (9)$$

where E is a positive operator (or POVM element). A similar maximisation over states in turn induces a distance on quantum *channels*, defined as

$$\|\mathcal{E}_A - \mathcal{E}_B\|_{\diamond,1} = \max_{\rho \in S} \|(\mathcal{E}_A \otimes \mathbb{I})(\rho) - (\mathcal{E}_B \otimes \mathbb{I})(\rho)\|. \quad (10)$$

The associated task is to submit an optimal initial state ρ to undergo evolution under \mathcal{E}_A or \mathcal{E}_B (chosen at random), and to perform the state discrimination task (above) on the output state. For full generality the enlarged search space S (having dimensions d^2) is needed to allow for the possibility of entanglement with an ancilla (of dimension no larger than that defined by the channels themselves) assisting in the channel discrimination task [37]. When the full search space S is available, $\|\cdot\|_{\diamond}$ is the diamond norm [37]; otherwise, when the maximization is over states which factorize into system, ancilla states, the norm is the unstabilized induced trace-norm $\|\cdot\|_1$ (and the ancilla plays no role). A further restriction considered by Lloyd [22] would be to define the set of states of ‘interest’ S_{int} : but this has the drawback of requiring detailed knowledge of the particular simulation at hand,

and makes additional assumptions on the set of initial states of interest: see Figure 1.

These metrics then gives the bias away from a half in the probability of discriminating between the real and ideal channels, given a single optimal initial state preparation (for the diamond norm over a larger space), a single channel use and a single sample from an optimally chosen measurement basis (again for the diamond norm on a larger space):

$$p_{\text{distinguish}} \leq \frac{1}{2} + \frac{1}{4} \|\mathcal{E}_A - \mathcal{E}_B\|_{\diamond,1}. \quad (11)$$

They are therefore worst-case metrics. Yet another norm to consider is the J -norm $\|\cdot\|_J$: this provides a bound on the average trace distance over a uniformly measured state space [38]. The J -distance between two quantum maps is merely the trace distance of the associated states in the Jamiolkowski isomorphism [39]:

$$\|\mathcal{E}_A - \mathcal{E}_B\|_J = \|J(\mathcal{E}_A) - J(\mathcal{E}_B)\|, \quad (12)$$

where $J(\mathcal{E}) \propto \sum_{ij} \mathcal{E}(|i\rangle\langle j|) \otimes |i\rangle\langle j|$ with the constant of proportionality such that $J(\mathcal{E})$ has unit trace. The J -distance is related to the average probability of discriminating the real and ideal simulations, given an optimal measurement:

$$\bar{p}_{\text{distinguish}} \leq \frac{1}{2} + \frac{1}{4} \|\mathcal{E}_A - \mathcal{E}_B\|_J. \quad (13)$$

For a comprehensive survey of available metrics, see Ref. [38] [40].

There are a number of senses in which these metrics are pessimistic measures. Firstly, the maximisation over POVMs: in reality, the measurements are likely to be restricted to those revealing macroscopic observables, e.g. the ground state energy of the system, the Shannon entropy, effective temperature, net magnetisation and so on. Consider that these measurement choices might be completely impervious to certain types of error, but yet the errors are ruthlessly sought out and exposed under the trace-norm or diamond-norm distances. Secondly, a final state that is distinguishable from the ideal with high probability is not necessarily very inaccurate: in a very large simulator, a bit-flip error on a single qubit can be enough to realise the worst-case $p_{\text{distinguish}} = 1$, but yet the extracted data may be extremely precise, perhaps providing scalars differing from the ideal in only the 7th or 8th significant digit (for example). Thirdly, for the worst-case metrics, an optimal input state (possibly entangled with an ancilla) may not arise in a quantum simulator: readout methods such as the phase estimation algorithm [41], for example, do not employ such entangled states. Currently, the full set of preparations and measurements at the disposal of a quantum computer are not made use of: in the future procedures including readout using an ancilla may turn out to be more powerful at extracting information from quantum simulators. The game of simulation is not necessarily an adversarial

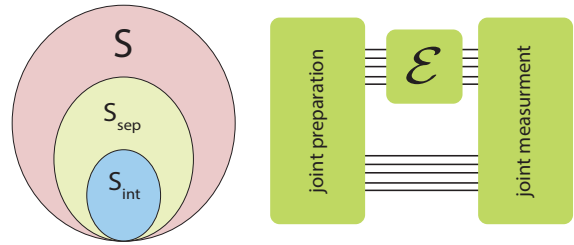


FIG. 1. Should the induced trace norm distance maximize over the entire enlarged space or merely over product states? Or even over a smaller set of interesting states? The worst-case scenario involves entanglement with an ancilla.

one – nevertheless the worst-case metrics are usually regarded as the most elegant and fair measures to employ.

All metrics satisfy some important properties which we will make use of: the triangle inequality $\|\mathcal{E}_A - \mathcal{E}_C\| \leq \|\mathcal{E}_A - \mathcal{E}_B\| + \|\mathcal{E}_B - \mathcal{E}_C\|$ and convexity $\|\sum_i p_i \mathcal{E}_i\| \leq \sum_i p_i \|\mathcal{E}_i\|$. Another important property satisfied by all metrics considered in this paper is chaining: $\|\mathcal{E}_{A_1} \circ \mathcal{E}_{A_2} - \mathcal{E}_{B_1} \circ \mathcal{E}_{B_2}\| \leq \|\mathcal{E}_{A_1} - \mathcal{E}_{B_1}\| + \|\mathcal{E}_{A_2} - \mathcal{E}_{B_2}\|$. The diamond norm and J distance are special in that they are *stable*: they satisfy $\|\mathbb{I} \otimes \mathcal{E}\|_{\diamond,J} = \|\mathcal{E}\|_{\diamond,J}$.

The convexity property is an important one, and is enough to ensure that the maximum statistical distance is achieved on a pure state [38]. Further, although often understood as the inability to increase distinguishability through averaging (i.e. as a handicap in information processing tasks such as parameter estimation [42]), here it implies that the performance of a faulty quantum computation may be *improved* by repeating the computation and averaging the results. As we shall see below, this can lead to quite significant improvements, because the fluctuations may be suppressed.

VI. THE COMPLETELY NOISY BENCHMARK

A related fact concerns appropriate worst-case benchmarks. Whilst the ideal evolution \mathcal{U} is unitary and will take a pure state to a pure state, a completely noisy channel $\mathcal{E}^{\rho \rightarrow \mathbb{I}/d}(\rho) = \mathbb{I}/d$ destroys the purity of any state (having dimension d). One can prove [43] that under the unstabilised trace norm one has

$$\|\mathcal{E}^{\rho \rightarrow \mathbb{I}/d} - \mathcal{U}\|_1 = 2 - \frac{2}{d} \quad (14)$$

whereas the diamond norm [44] and J -distance (which we concentrate on for the remainder of this article) one has

$$\|\mathcal{E}^{\rho \rightarrow \mathbb{I}/d} - \mathcal{U}\|_{\diamond,J} = 2 - \frac{2}{d^2}. \quad (15)$$

These values represent benchmarks – the distinguishability between the output of the ideal simulation and complete noise. Any simulation giving a higher distance

that this will be worse than a completely random output! In the examples studied in this paper, one observes the metrics saturating to these quantities, suggesting that the ‘steady state’ ($n \rightarrow \infty$) map is the completely noisy map. Note that both norms converge to the algebraic maximum of 2 as $d \rightarrow \infty$.

VII. RESULTS

We are now in a position to calculate the accuracy of a realistic quantum simulator. To that end, we apply the norms introduced above to calculate the statistical distance from the ideal map to the faulty Trotter map. To see why we expect an optimum Trotter number to emerge in realistic universal quantum simulators, consider first a simple application of the triangle inequality:

$$\left\| \sqrt[n]{\mathcal{U}} - \mathcal{E}^{\text{fTss}} \right\| \leq \left\| \sqrt[n]{\mathcal{U}} - \sqrt[n]{\mathcal{V}} \right\| + \left\| \sqrt[n]{\mathcal{V}} - \mathcal{E}^{\text{fTss}} \right\|. \quad (16)$$

Next, assume the first term is bounded by a quantity $\propto n^{-s}$ for some $s \geq 2$: this captures the first order Trotter formula that we study here ($s = 2$), as well as higher order expansions [26]. Now assume the second term is a constant w.r.t n . This immediately leads, via the chaining property, to

$$\left\| \mathcal{U} - \mathcal{E}^{\text{faultyTrotter}} \right\| \leq \frac{\mathcal{C}}{n^{s-1}} + \mathcal{D}n \quad (17)$$

for some constants of proportionality \mathcal{C} and \mathcal{D} . By inspection this function exhibits a minimum at some n^* . Below we investigate some particular noise models that influence the constants \mathcal{C} and \mathcal{D} .

A. Mistimed control

Trotterization fundamentally requires ‘switching’ between unitary gates: in our simplification this is thought of as switching each component Hamiltonian H_j on for a specific duration. Consider that the duration is increased (decreased) by a random number Δ_{ij} , normally distributed around zero with variance σ^2 . This makes

$$\mathcal{E}_{ij}^{\text{MTC}}(\rho) = e^{iH_i\Delta_{ij}} \rho e^{-iH_i\Delta_{ij}}. \quad (18)$$

Such imperfection is ubiquitous in the control of quantum systems, and an equivalent imperfection (laser intensity fluctuations) was cited as the dominant error source by Lanyon et al. in a recent implementation of universal quantum simulation [4]. Under this noise model, the total map $\mathcal{E}^{\text{faultyTrotter}}$, being a concatenation of random unitaries, is itself a random unitary map. Note that the magnitude of the errant time-shift Δ_{ij} is independent of t or n , but the error map is more severe when $\|H_i\|$ is large, i.e. the simulator is driven ‘hard’.

As shown in the supplementary material [45], by assuming $\|H_i[t/n + \Delta_{ij}]\| \ll 1$ one can find the difference between real and ideal supermatrices for this error model, finding

$$\begin{aligned} \sqrt[n]{\mathcal{U}} - \mathbf{T}_i^{\text{fTss}} &= \sum_{j>l} (\mathbb{I} \otimes [H_j^*, H_l^*] + [H_j, H_l] \otimes \mathbb{I}) \frac{t^2}{2n^2} + \sum_j (\mathbb{I} \otimes H_j^* + H_j \otimes \mathbb{I}) \Delta_{ij} \\ &+ \sum_{k < m} (\mathbb{I} \otimes H_k^* H_m^* + H_k H_m \otimes \mathbb{I}) \left[\frac{t}{n} \Delta_{ik} + \frac{t}{n} \Delta_{im} + \Delta_{ik} \Delta_{im} \right] + \frac{1}{2} \sum_k (\mathbb{I} \otimes H_k^{2*} + H_k^2 \otimes \mathbb{I}) \left[2 \frac{t}{n} \Delta_{ik} + \Delta_{ik}^2 \right] \\ &- \sum_{jk} H_j \otimes H_k^* \left[\frac{t}{n} \Delta_{ij} + \frac{t}{n} \Delta_{ik} + \Delta_{ij} \Delta_{ik} \right] + \dots \end{aligned} \quad (19)$$

Note that the terms linear in Δ work to introduce ‘coherent’ or reversible errors that may be averaged away because of our assumptions $\Delta_{ij} = 0$ and $\Delta_{ik} \Delta_{im} = \delta_{km} \sigma^2$, hence

$$\begin{aligned} \overline{\sqrt[n]{\mathcal{U}} - \mathbf{T}_i^{\text{fTss}}} &= \sum_{i>l} (\mathbb{I} \otimes [H_i^*, H_l^*] + [H_i, H_l] \otimes \mathbb{I}) \frac{t^2}{2n^2} \\ &+ \frac{1}{2} \sum_k (\mathbb{I} \otimes H_k^{2*} + H_k^2 \otimes \mathbb{I}) \sigma^2 \\ &- \sum_k (H_k \otimes H_k^*) \sigma^2 + \dots \end{aligned} \quad (20)$$

leaving the ‘incoherent’ or irreversible errors (quadratic

in Δ) remaining. Clearly averaging can help reduce fluctuations introduced by the noise. Figure 2 shows (through numerical simulations) how averaging can reduce the simulation error for this noise model, as measured by the diamond norm distance. Taking the norm of (20) gives the statistical distance, and employing the triangle inequality gives

$$D_{\text{MTC}}^{ss} \lesssim \mathcal{A} \frac{t^2}{2n^2} + \mathcal{B} \sigma^2. \quad (21)$$

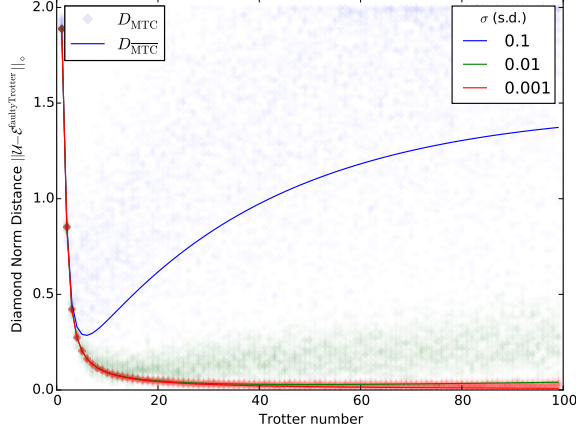


FIG. 2. Diamond norm distance versus Trotter number. Note how averaging reduces the statistical distance: each circle represents a single monte-carlo simulated random unitary evolution of the simulator. The lines represent the averaged map. Note how the position of the averaged map is far below the average position of the dots (mean position not explicitly marked). The performance of the average map is better than the average performance of the maps of which it is composed. The various colours correspond to different noise characteristics of the mistimed Hamiltonian noise model. The Hamiltonian is $H = \sigma_x + \sigma_y$.

By the chaining property we reach

$$D_{\overline{\text{MTC}}} \lesssim \mathcal{A} \frac{t^2}{2n} + \mathcal{B} n \sigma^2 \quad (22)$$

with

$$\begin{aligned} \mathcal{A} &= \left\| \sum_{i < l} (\mathbb{I} \otimes [H_i, H_l]^* + [H_i, H_l] \otimes \mathbb{I}) \right\|_? \\ \mathcal{B} &= \left\| \frac{1}{2} \sum_i \left(\mathbb{I} \otimes H_i^{*2} + H_i^2 \otimes \mathbb{I} - 2H_i \otimes H_i^* \right) \right\|_? \end{aligned} \quad (23)$$

Note that we leave the choice of norm free here: $? \in \{\diamond, 1, J, \dots\}$. We only made use of the triangle inequality and the chaining property. As we will show, if $\mathcal{A} : \mathcal{B}$ happens to be invariant under choice of norm the optimum Trotter number is also an invariant, since it only depends on this ratio.

Taking $n \in \mathbb{N}$ for the moment, simple analysis yields i) the optimum Trotter number

$$n_{\overline{\text{MTC}}}^* = \sqrt{\mathcal{A}(2\mathcal{B})^{-1}} t \sigma^{-1}, \quad (24)$$

ii) the statistical distance at this optimum

$$D_{\overline{\text{MTC}}}(n^*) = \sqrt{2\mathcal{A}\mathcal{B}t\sigma} \quad (25)$$

and iii) the maximum simulation time after which the DND is above the accepted level D_{\max} , given by

$$t_{\max} = D_{\max} / (\sigma \sqrt{2\mathcal{A}\mathcal{B}}). \quad (26)$$

The meaning of equations (24),(25) and (26) is inherited from the choice of norm in the definition of \mathcal{A} and \mathcal{B} .

Of course in reality $n^* \in \mathbb{Z}$: the true optimum must be a whole number of Trotter steps, and so n^* should be rounded in the direction of the sign of $\lfloor n^* \rfloor \lceil n^* \rceil - \mathcal{A}t^2/(2\mathcal{B}\sigma^2)$. See [45] for more details.

Although our formulae apply generally, as a case study we study the Ising Hamiltonian

$$H_1 = \sum_j^N \sigma_z^j \quad (27)$$

$$H_2 = \sum_{\langle i,j \rangle} \sigma_x^i \sigma_x^j \quad (28)$$

with σ_x^i and σ_z^i the Pauli matrices acting on qubit i of N , with identity matrices implied on other qubits. The notation $\sum_{\langle i,j \rangle}$ denotes a sum over nearest neighbours. Note that $[H_1, H_2] \neq 0$. As shown in Figure 3, our approximate analytical upper bound (22) is a good fit for exact numerics in the correct parameter regime (for example we chose $t = 0.1$ and $N = 2$).

We note three regimes where the fit is worse: i) when $\|H_i t/n\| \approx 1$ (the perturbative expansion breaks down), ii) in the tradeoff region near the optimum Trotter number n^* (here the chaining inequality is loose) and iii) when the distance measure approaches its maximum (the errors are saturating, and the chaining inequality between consecutive Trotter steps is loose). Despite the looseness of the fit in these areas, the location of n^* is well captured, and $D(n^*)$ seems accurate to within a constant factor (of order 2).

A number of comments are in order. According to (25), the best performance one can hope to achieve is proportional to the characteristic of the noise – this means that in order to improve the performance by a factor of f , the standard deviation of the noise must be reduced by f . Aside from combatting the gate noise via averaging, one can apply the time-energy freedom (3), noting that

$$a \neq 1 \Rightarrow D_{\overline{\text{MTC}}} \lesssim \mathcal{A} \frac{t^2}{2n} + \mathcal{B} n (a\sigma)^2. \quad (29)$$

Clearly one can now take $a < 1$, i.e. retard the simulator to decrease the absolute error at each Trotter step. This has the same effect as reducing σ – the first term is unaffected.

B. Trotter step induced depolarisation

Next we study a different noise model. Depolarising noise is commonly used to phenomenologically model noise because it makes analytic results tractable. To gain an idea of how each operation might introduce generic noise into the simulator, we assume that after a single Trotter step the combined effect of imperfections in the

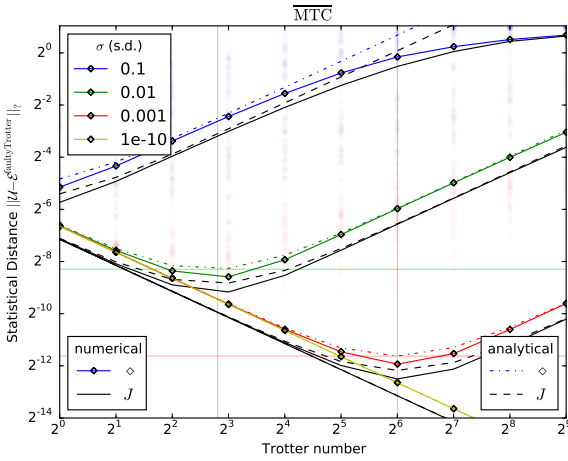


FIG. 3. Log-Log plot of the statistical distance versus the Trotter number for the MTC noise model. Transparent circles are each an independent Monte Carlo run, calculated numerically with the diamond norm (lower is better). Solid lines (numerically calculated) correspond to the averaged map. The dotted lines are approximate analytical formulae relating to the averaged map. Note the improved performance of the averaged strategy. The different colours correspond to the standard deviation σ of the noise, shown in the legend. Black lines are the J -distance (solid line are exact numerics, dotted lines are approximate analytics). The crosshairs show the analytically predicted optimum Trotter number and performance level at that optimum.

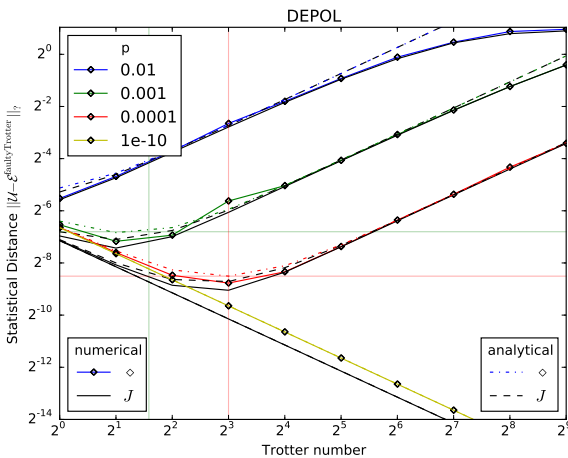


FIG. 4. Log-Log plot of the diamond norm Distance versus the Trotter number for the DEPOL noise model. Solid lines are numerically calculated with the superoperator (averaged) map. The different colours correspond to the noise characteristic p shown in the legend. The crosshairs show the analytically predicted optimum Trotter number and performance level at that optimum.

applied gates is to depolarise the entire simulator uni-

formly. The faulty map is then

$$\mathcal{E}^{\text{faultyTrotter}}(\rho) = \bigcirc_i \mathcal{E}_i^{\text{DEPOL}} \circ (\dots \mathcal{V}_2 \circ \mathcal{V}_1)(\rho) \quad (30)$$

$$= \bigcirc_i \mathcal{E}_i^{\text{fTss}} \quad (31)$$

with

$$\mathcal{E}_i^{\text{DEPOL}}(\rho) = (1 - p)\rho + \frac{p}{d} \mathbb{I}. \quad (32)$$

Here \mathbb{I} is the $d \times d$ identity matrix. Note there is no dependence on any variable other than p , which captures the severity of the noise. Now

$$\begin{aligned} \mathcal{E}^{\text{fTss}} - \sqrt[n]{\mathcal{U}} &= (1 - p) \sqrt[n]{\mathcal{V}} \\ &\quad + p \mathcal{E}^{\rho \rightarrow \mathbb{I}/d} - \sqrt[n]{\mathcal{U}} \\ &= (1 - p) \left[\sqrt[n]{\mathcal{V}} - \sqrt[n]{\mathcal{U}} \right] \\ &\quad + p \left[\mathcal{E}^{\rho \rightarrow \mathbb{I}/d} - \sqrt[n]{\mathcal{U}} \right], \end{aligned} \quad (33)$$

and we can use convexity to reach

$$\begin{aligned} \left\| \mathcal{E}^{\text{fTss}} - \sqrt[n]{\mathcal{U}} \right\| &\leq (1 - p) \left\| \sqrt[n]{\mathcal{V}} - \sqrt[n]{\mathcal{U}} \right\| \\ &\quad + p \left\| \mathcal{E}^{\rho \rightarrow \mathbb{I}/d} - \sqrt[n]{\mathcal{U}} \right\|. \end{aligned} \quad (34)$$

Now the first term follows trivially from the above calculation and equals $(1 - p) D_{\text{MTC}}^{\text{ss}} \Big|_{\sigma=0}$. The second term is also known (see above). This means that (again employing the chaining inequality over the n iterations of the single step channel, and assuming $\|H_i\| t/n \ll 1$)

$$D_{\text{DEPOL}} \lesssim (1 - p) \mathcal{A} \frac{t^2}{2n} + np \left(2 - \frac{2}{d^2} \right) \quad (35)$$

which we can simplify, in the case of $d \gg 1$ to

$$D_{\text{DEPOL}} \lesssim (1 - p) \mathcal{A} \frac{t^2}{2n} + 2pn. \quad (36)$$

Qualitatively this is very similar to the MTC model. One cannot however leverage the freedom in the time-energy correspondence to effectively reduce p , the characteristic of the noise, because (36) is invariant under that transformation. One has

$$n_{\text{DEPOL}}^* = t \sqrt{\frac{(1 - p) \mathcal{A}}{2p(2 - \frac{2}{d^2})}} \quad (37)$$

or in the case of $d \gg 1$

$$n_{\text{DEPOL}}^* = t \sqrt{\frac{(1 - p) \mathcal{A}}{4p}}. \quad (38)$$

Note that, as with above, one should round n^* to the nearest integer in the direction of the sign of $\lfloor n^* \rfloor \lceil n^* \rceil - (1 - p) \mathcal{A} t^2 / 4p$ [45]. One has

$$D_{\text{DEPOL}}(n^*) = 2t \sqrt{\mathcal{A}(1 - p)}. \quad (39)$$

See Figure 4 for comparison with numerical results.

C. Decoherence

To model the overall noise of a simulator under perfect control, we depolarise the simulator in a manner that is independent of the number of operations. This means the number of Trotter steps does not affect the total noise characteristics. A very similar argument to the above gives

$$\begin{aligned} \mathcal{E}^{\text{faultyTrotter}} - \mathcal{U} = & (1 - p(t))[\mathcal{V} - \mathcal{U}] \\ & + p(t)[\mathcal{E}^{p \rightarrow \mathbb{I}/d} - \mathcal{U}] \end{aligned} \quad (40)$$

and now $p(t)$ increases over time. Typically $1 - p(t)$ represents exponential decay of population and coherence with time [42]. The first term follows trivially and is equal to $(1 - p) D_{\text{MTC}}|_{\sigma=0}$. We have

$$D_{\text{DECOH}} \leq (1 - p(t)) \frac{\mathcal{A}t^2}{2n} + p(t) \left(2 - \frac{2}{d^2} \right) \quad (41)$$

Once more employing the time energy freedom (3) we find

$$D_{\text{DECOH}} \leq \left(1 - p \left(\frac{t}{a} \right) \right) \frac{\mathcal{A}t^2}{2n} + p \left(\frac{t}{a} \right) \left(2 - \frac{2}{d^2} \right); \quad (42)$$

note that accelerating the simulator $a > 1$ will improve performance if $p(t)$ is monotonically increasing. Note here there is no optimum Trotter number, because the noise is not worsened by increasing the number of operations.

VIII. DISCUSSION

By modelling some simple imperfections in the control of a Trotterized universal quantum simulator, we have

shown how the accuracy of the quantum channel that is applied depends on various parameters. These parameters include those outside of direct experimental control, such as the severity of environmental decoherence or the spread in control timing; and also controllable quantities such as the Trotter number and the simulator/simuland time ratio. We suggested ways in which these quantities can be optimised over in order to improve the accuracy of the simulation, which we quantified by calculating the statistical distance to the ideal map. The optimisation implies only that the uncontrollable quantities be estimated from control experiments, and that \mathcal{A} and \mathcal{B} be calculated only once (possibly numerically). We discussed the choice of a number of norms for this purpose, including the worst-case induced-trace norm and stabilised (diamond) norm, as well as the average-case J-distance.

In particular we found there to be an finite optimum Trotter number to employ, setting a maximum performance and a maximum simulation time. By way of a general argument, we have shown these features to be generic to faulty simulators operated with a Trotterized (or similar) algorithm. Future work will investigate the multiparameter optimisation when all noise types are present, the use of alternative Trotter-type approximants, and the performance of simulators when the set of interesting states and applied measurements is chosen from a restricted set.

ACKNOWLEDGMENTS

We thank Yuichiro Matsuzaki and Kae Nemoto for helpful discussions.

[1] G. E. Moore, *Electronics* **38**, 114 (1965).

[2] I. Kassal, J. D. Whitfield, A. Perdomo-Ortiz, M.-H. Yung, and A. Aspuru-Guzik, *Annual Review of Physical Chemistry* **62**, 185 (2011).

[3] R. Barends, L. Lamata, J. Kelly, L. García-Álvarez, A. G. Fowler, A. Megrant, E. Jeffrey, T. C. White, D. Sank, J. Y. Mutus, B. Campbell, Y. Chen, Z. Chen, B. Chiaro, A. Dunsworth, I. C. Hoi, C. Neill, P. J. J. O’Malley, C. Quintana, P. Roushan, A. Vainsencher, J. Wenner, E. Solano, and J. M. Martinis, (2015), arXiv:1501.07703v1 [quant-ph].

[4] B. P. Lanyon, C. Hempel, D. Nigg, M. Müller, R. Gerritsma, F. Zähringer, P. Schindler, J. T. Barreiro, M. Rambach, G. Kirchmair, M. Hennrich, P. Zoller, R. Blatt, and C. F. Roos, *Science* **334**, 57 (2011).

[5] X.-s. Ma, B. Dakic, W. Naylor, A. Zeilinger, and P. Walther, *Nat Phys* **7**, 399 (2011).

[6] U. L. Heras, A. Mezzacapo, L. Lamata, S. Filipp, A. Wallraff, and E. Solano, *Phys. Rev. Lett.* **112**, 200501 (2014).

[7] I. M. Georgescu, S. Ashhab, and F. Nori, *Rev. Mod. Phys.* **86**, 153 (2014).

[8] D. Deutsch, *Proceedings of the Royal Society of London A: Mathematical, Physical and Engineering Sciences* **425**, 73 (1989).

[9] A. Barenco, C. Bennett, R. Cleve, D. DiVincenzo, N. Margolus, P. Shor, T. Sleator, J. Smolin, and H. Weinfurter, *Phys. Rev. A* **52**, 3457 (1995).

[10] D. Deutsch, A. Barenco, and A. Ekert, *Proceedings of the Royal Society of London. Series A: Mathematical and Physical Sciences* **449**, 669 (1995).

[11] S. Lloyd, *Phys. Rev. Lett.* **75**, 346 (1995).

[12] T. D. Ladd, F. Jelezko, R. Laflamme, Y. Nakamura, C. Monroe, and J. L. O’Brien, *Nature* **464**, 45 (2010).

[13] I. Buluta and F. Nori, *Science* **326**, 108 (2009).

- [14] N. Zuniga-Hansen, Y.-C. Chi, and M. S. Byrd, Phys. Rev. A **86**, 042335 (2012).
- [15] A. Peruzzo, J. McClean, P. Shadbolt, M.-H. Yung, X.-Q. Zhou, P. J. Love, A. Aspuru-Guzik, and J. L. O’Brien, (2013), arXiv:1304.3061v1 [quant-ph].
- [16] D. Aharonov and M. Ben-Or, in *Proceedings of the Twenty-ninth Annual ACM Symposium on Theory of Computing*, STOC ’97 (ACM, New York, NY, USA, 1997) pp. 176–188.
- [17] A. Y. Kitaev, Russian Mathematical Surveys **52**, 1191 (1997).
- [18] P. Aliferis, D. Gottesman, and J. Preskill, Quantum Info. Comput. **6**, 97 (2006).
- [19] E. Knill, R. Laflamme, and W. H. Zurek, Science **279**, 342 (1998).
- [20] B. M. Terhal, (2013), arXiv:1302.3428v5 [quant-ph].
- [21] B. P. Lanyon, J. D. Whitfield, G. G. Gillett, M. E. Goggin, M. P. Almeida, I. Kassal, J. D. Biamonte, M. Mohseni, B. J. Powell, M. Barbieri, A. Aspuru-Guzik, and A. G. White, Nat Chem **2**, 106 (2010).
- [22] S. Lloyd, Science **273**, 1073 (1996).
- [23] H. F. Trotter, Proc. Amer. Math. Soc. **10**, 545 (1959).
- [24] K. L. Brown, W. J. Munro, and V. M. Kendon, Entropy **12**, 2268 (2010).
- [25] K. R. Brown, R. J. Clark, and I. L. Chuang, Phys. Rev. Lett. **97**, 050504 (2006).
- [26] W. Janke and T. Sauer, Physics Letters A **165**, 199 (1992).
- [27] M. Suzuki, Physics Letters A **165**, 387 (1992).
- [28] D. Berry, G. Ahokas, R. Cleve, and B. Sanders, Communications in Mathematical Physics **270**, 359 (2007), 10.1007/s00220-006-0150-x.
- [29] D. Poulin, M. B. Hastings, D. Wecker, N. Wiebe, A. C. Doherty, and M. Troyer, (2014), arXiv:1406.4920v1 [quant-ph].
- [30] D. Wecker, B. Bauer, B. K. Clark, M. B. Hastings, and M. Troyer, Phys. Rev. A **90**, 022305 (2014).
- [31] A simulator cannot be operated in sublinear time: that is, it cannot take less than a time proportional to t_{simuland} [28].
- [32] M. Reed and B. Simon, *Methods of Modern Mathematical Physics: Functional analysis*, Methods of Modern Mathematical Physics No. v. 1 (Academic Press, 1980).
- [33] I. Dhand and B. C. Sanders, Journal of Physics A: Mathematical and Theoretical **47**, 265206 (2014).
- [34] W. Dür, M. J. Bremner, and H. J. Briegel, Phys. Rev. A **78**, 052325 (2008).
- [35] P. Hauke, F. M. Cucchietti, L. Tagliacozzo, I. Deutsch, and M. Lewenstein, (2011), 1109.6457v2.
- [36] C. A. Fuchs, (1996), arXiv:quant-ph/9601020v1 [quant-ph].
- [37] A. Kitaev, A. Shen, and M. Vyalyi, *Classical and Quantum Computation*, Graduate studies in mathematics (American Mathematical Society, 2002).
- [38] A. Gilchrist, N. K. Langford, and M. A. Nielsen, Phys. Rev. A **71**, 062310 (2005).
- [39] A. Jamiolkowski, Reports on Mathematical Physics **3**, 275 (1972).
- [40] In [38] they refer to the diamond norm as the S -distance.
- [41] A. Aspuru-Guzik, A. D. Dutoi, P. J. Love, and M. Head-Gordon, Science **309**, 1704 (2005).
- [42] M. Nielsen and I. Chuang, *Quantum Computation and Quantum Information (Cambridge Series on Information and the Natural Sciences)*, 1st ed. (Cambridge University Press, 2004).
- [43] Due to the property of unitary invariance we can assume here that the unitary channel is the identity channel.
- [44] M. Sacchi, Phys. Rev. A **71**, 062340 (2005).
- [45] “Supplementary material.”.